Molecular Psychiatry (2013), 1–9

www.nature.com/mp

ORIGINAL ARTICLE

The autism brain imaging data exchange: towards a large-scale evaluation of the intrinsic brain architecture in autism

A Di Martino[1], C-G Yan[2,39], Q Li[3,39], E Denio[1], FX Castellanos[1,2], K Alaerts[1,4], JS Anderson[5,6,7,8], M Assaf[9,10], SY Bookheimer[11,12,13,14], M Dapretto[12,13,15], B Deen[10,16], S Delmonte[17], I Dinstein[18,19], B Ertl-Wagner[20], DA Fair[21], L Gallagher[17], DP Kennedy[22,23], CL Keown[24], C Keysers[25,26], JE Lainhart[27,28], C Lord[29], B Luna[30], V Menon[31], NJ Minshew[32], CS Monk[33], S Mueller[20], R-A Müller[24], MB Nebel[34], JT Nigg[35], K O'Hearn[30], KA Pelphrey[10], SJ Peltier[33], JD Rudie[12,13,14,15], S Sunaert[36], M Thioux[25,26], JM Tyszka[37], LQ Uddin[31], JS Verhoeven[36], N Wenderoth[4], JL Wiggins[33], SH Mostofsky[34,38] and MP Milham[2,3]

Autism spectrum disorders (ASDs) represent a formidable challenge for psychiatry and neuroscience because of their high prevalence, lifelong nature, complexity and substantial heterogeneity. Facing these obstacles requires large-scale multidisciplinary efforts. Although the field of genetics has pioneered data sharing for these reasons, neuroimaging had not kept pace. In response, we introduce the Autism Brain Imaging Data Exchange (ABIDE)—a grassroots consortium aggregating and openly sharing 1112 existing resting-state functional magnetic resonance imaging (R-fMRI) data sets with corresponding structural MRI and phenotypic information from 539 individuals with ASDs and 573 age-matched typical controls (TCs; 7–64 years) (http://fcon_1000.projects.nitrc.org/indi/abide/). Here, we present this resource and demonstrate its suitability for advancing knowledge of ASD neurobiology based on analyses of 360 male subjects with ASDs and 403 male age-matched TCs. We focused on whole-brain intrinsic functional connectivity and also survey a range of voxel-wise measures of intrinsic functional brain architecture. Whole-brain analyses reconciled seemingly disparate themes of both hypo- and hyperconnectivity in the ASD literature; both were detected, although hypoconnectivity dominated, particularly for corticocortical and interhemispheric functional connectivity. Exploratory analyses using an array of regional metrics of intrinsic brain function converged on common loci of dysfunction in ASDs (mid- and posterior insula and posterior cingulate cortex), and highlighted less commonly explored regions such as the thalamus. The survey of the ABIDE R-fMRI data sets provides unprecedented demonstrations of both replication and novel discovery. By pooling multiple international data sets, ABIDE is expected to accelerate the pace of discovery setting the stage for the next generation of ASD studies.

Molecular Psychiatry advance online publication, 18 June 2013; doi:10.1038/mp.2013.78

Keywords: data sharing; default network; interhemispheric connectivity; intrinsic functional connectivity; resting-state fMRI; thalamus

INTRODUCTION

Autism spectrum disorders (ASDs), formerly considered rare, are now reported to occur in ~1% of children.[1,2] Increased recognition of ASDs derives at least partially from the adoption of standardized methods for their evaluation and diagnosis.[3,4] Beyond clinical utility, standardized approaches facilitate comparison and synthesis of findings across research studies. Consistent phenotypic characterizations have also facilitated

[1]Phyllis Green and Randolph Cowen Institute for Pediatric Neuroscience at the NYU Child Study Center, New York University Langone Medical Center, New York, NY, USA; [2]Nathan S Kline Institute for Psychiatric Research, Orangeburg, NY, USA; [3]Center for the Developing Brain, Child Mind Institute, New York, NY, USA; [4]KU Leuven, Leuven, Belgium; [5]Division of Neuroradiology, University of Utah, Salt Lake City, UT, USA; [6]Interdepartmental Program in Neuroscience, University of Utah, Salt Lake City, UT, USA; [7]The Brain Institute at the University of Utah, Salt Lake City, UT, USA; [8]Department of Bioengineering, University of Utah, Salt Lake City, UT, USA; [9]Olin Neuropsychiatry Research Center, Institute of Living at Hartford Hospital, Hartford, CT, USA; [10]Yale School of Medicine, New Haven, CT, USA; [11]Center for Cognitive Neuroscience, UCLA, Los Angeles, CA, USA; [12]Department of Psychiatry and Biobehavioral Sciences, Semel Institute for Neuroscience and Human Behavior, UCLA, Los Angeles, CA, USA; [13]Interdepartmental Neuroscience Program, UCLA, Los Angeles, CA, USA; [14]David Geffen School of Medicine, UCLA, Los Angeles, CA, USA; [15]Ahmanson-Lovelace Brain Mapping Center, UCLA, Los Angeles, CA, USA; [16]Department of Brain and Cognitive Sciences, Massachusetts Institute of Technology, Cambridge, MA, USA; [17]Department of Psychiatry and Trinity College Institute of Neuroscience, Trinity College Dublin, Dublin, UK; [18]Department of Psychology, Carnegie Mellon University, Pittsburgh, PA, USA; [19]Psychology, Ben Gurion University of the Negev, Beersheba, Israel; [20]Institute for Clinical Radiology, Ludwig Maximilians University Munich, Munich, Germany; [21]Behavioral Neuroscience and Psychiatry Departments, and Advanced Imaging Research Center, Oregon Health and Science University, Portland, OR, USA; [22]Division of Humanities and Social Sciences, California Institute of Technology, Pasadena, CA, USA; [23]Department of Psychological and Brain Sciences, Indiana University, Bloomington, IN, USA; [24]Department of Psychology, San Diego State University, San Diego, CA, USA; [25]Netherlands Institute for Neuroscience, Royal Dutch Academy of Science (KNAW), Amsterdam, The Netherlands; [26]BCN NeuroImaging Center, University Medical Center Groningen, Rijksuniversiteit Groningen, Groningen, The Netherlands; [27]Waisman Laboratory for Brain Imaging and Behavior, University of Wisconsin, Madison, WI, USA; [28]Department of Psychiatry, Division of Child and Adolescent Psychiatry, University of Wisconsin, Madison, WI, USA; [29]Weill-Cornell Medical College, New York, NY, USA; [30]University of Pittsburgh School of Medicine, Pittsburgh, PA, USA; [31]Stanford University, Stanford, CA, USA; [32]Departments of Psychiatry and Neurology, University of Pittsburgh, Pittsburgh, PA, USA; [33]University of Michigan, Ann Arbor, MI, USA; [34]Laboratory for Neurocognitive and Imaging Research, Kennedy Krieger Institute, Baltimore, MD, USA; [35]Oregon Health and Science University, Portland, OR, USA; [36]Translational MRI, University of Leuven (KU Leuven), Leuven, Belgium; [37]Division of Biology, Caltech, Pasadena, CA, USA and [38]Departments of Neurology and Psychiatry, Johns Hopkins School of Medicine, Baltimore, MD, USA. Correspondence: Dr A Di Martino, Phyllis Green and Randolph Cowen Institute for Pediatric Neuroscience at the NYU Child Study Center, New York University Langone Medical Center, One Park Avenue, 8th Floor New York, NY 10016, USA or Dr MP Milham, Center for the Developing Brain, Child Mind Institute, 445 Park Avenue, New York, NY 10022, USA.
E-mail: dimara01@nyumc.org or michael.milham@childmind.org
[39]C-GY and QL contributed equally to this work.
Received 14 December 2012; revised 20 March 2013; accepted 19 April 2013

establishing large open access data repositories to address the genetic bases of ASDs.[5–8] Open sharing of neuroimaging data has not kept pace, despite substantial potential to inform our understanding of the neurophysiological mechanisms underlying autism.

In response, we introduce the Autism Brain Imaging Data Exchange (ABIDE; http://fcon_1000.projects.nitrc.org/indi/abide/)—a grassroots consortium effort dedicated to aggregating and sharing previously collected resting-state functional magnetic resonance imaging (R-fMRI) data sets from individuals with ASDs and age-matched typical controls (TCs). The focus on R-fMRI was motivated by multiple factors. First, ASD neuroimaging studies have increasingly converged on abnormalities in connectivity among brain regions, rather than local functional or structural abnormalities.[9–11] Second, R-fMRI approaches are particularly suitable for examining intrinsic functional connectivity (iFC); beyond robust test–retest reliability,[12,13] R-fMRI sidesteps the challenge of designing tasks capable of probing the wide range of intellectual and behavioral capabilities characteristic of ASDs.[14] Third, as recently demonstrated by the 1000 Functional Connectomes Project[15] and recent efforts from the International Neuroimaging Data-sharing Initiative (INDI; for example, the ADHD-200),[16–18] R-fMRI data sets from multiple imaging sites can be fruitfully aggregated for discovery and replication.[18,19]

In conceptualizing ABIDE, we hypothesized that the ASD community's adoption of standardized protocols would be reflected in the sample. Specifically, despite the lack of prior coordination, we expected comparable phenotyping across sites because of the widespread use of autism diagnostic standardized instruments.[3,4] We also anticipated identifying factors that vary across studies, whether by design or unintentionally, to guide future efforts to increase harmonization among research groups.

Another aim was to demonstrate the utility of the aggregated sample for exploring the functional connectome in ASDs. Despite overall convergence among R-fMRI studies in supporting a dysconnectivity model of ASDs, reports disagree regarding the specific nature and extent of ASD-related abnormalities in iFC (for example, hypo- vs hyperconnectivity) and the breadth of the systems affected.[20,21] In this work, we carry out a full-brain examination using parcellation unit-based correlation analyses to determine the relative prevalence of ASD-related increases vs decreases in iFC. Given the focus in the ASD literature on the default network,[22–25] we also examined voxel-wise iFC for its key components.[26]

Finally, we explored regional iFC dysfunction using four voxel-wise R-fMRI measures, regional homogeneity (ReHo),[27] voxel-matched homotopic connectivity (VMHC),[28,29] degree centrality (DC),[30,31] and fractional amplitude of low-frequency fluctuations (fALFF).[32] Neither fALFF, a direct index of the spontaneous signal fluctuations underlying resting-state functional connectivity, nor DC, a graph-based measure of the functional relationships of each voxel within the whole connectome, have been examined previously in ASDs. These approaches are suited for discovery science owing to their relative computational simplicity, lack of requirements for data reduction or *a priori* knowledge.

MATERIALS AND METHODS

Contributions

Initial contributions were sought from members of the ADHD-200 Consortium conducting autism research (Kennedy Krieger Institute, NYU Langone Medical Center, Oregon Health and Science University, University of Pittsburgh). Invitations to participate were extended based on personal communications, recent publications and conference presentations. All investigators willing and able to openly share previously collected awake R-fMRI data from individuals with ASDs and age- and sex-group matched TCs were included. Institutional Review Board's approval to participate, or explicit waiver to provide fully anonymized data, was required before data contribution.

All contributions were based on studies approved by the local Institutional Review Boards, and data were fully anonymized (removing all 18 HIPAA (Health Insurance Portability and Accountability)-protected health information identifiers, and face information from structural images). All data distributed were visually inspected before release.

Phenotypic data

Before data aggregation, consortium members agreed on a 'base' phenotypic protocol by identifying overlaps in measures across sites. These included age at scan, sex, IQ and diagnostic information. Contributors were encouraged to provide as many additional measures as possible, although such contributions were not required given the voluntary, unfunded nature of this effort.

Quality assurance. Upon receipt, data were checked for extreme outliers (relative to each site's group), impossible data entries (for example, beyond published maxima and minima) and missing values. Phenotypic variable entries (for example, diagnosis) were recoded as necessary to ensure uniformity across sites. Before distribution of quality-controlled data, each site reviewed and verified its accuracy. Missing data were imputed for each sample separately, based on individuals of the same diagnostic category, if the variable was present across $\geqslant$60% of data sets and sufficient data were available (that is, for $\geqslant$75% of participants in each diagnostic group at that site). Categorical variables were imputed using the mode and continuous variables using the mean per diagnostic group, per site. When missing, full IQ (FIQ) was estimated by averaging available performance and verbal IQ scores per diagnostic group, per site.

Surveying group characteristics. For continuous variables, we calculated range, mean and standard deviation (s.d.) for each diagnostic group per and across sites. Similarly, for categorical variables (for example, diagnosis per fourth and text revised edition of the Diagnostic and Statistical Manual of Mental Disorders (DSM-IV-TR)), we computed totals and percentages by diagnostic group.

Imaging analyses

Sample selection. Imaging analyses were limited to: (1) male subjects, as they represented 90% of the aggregate sample; (2) sites with IQ estimated for $>$75% per diagnostic group; (3) individuals with FIQ within 2 s.d. of the overall ABIDE sample mean (108 ± 15); (4) individuals with mean frame-wise displacement (FD)[33] $<$2 s.d. above the sample mean (0.23 ± 0.27 mm; Supplementary Figure 1); (5) data with anatomical images providing near-full brain coverage and successful registration; and (6) sites with at least 10 participants per group after the above exclusions. This yielded data for 763 individuals (ASDs = 360; TCs = 403) from 17 sites; (Supplementary Table 1).

Analytic strategy. Although the ASD literature converges on the presence of abnormal functional connectivity,[9,11] findings of hyper- vs hypoconnectivity vary across studies.[20] To understand the relative contributions of hypo- and hyperconnectivity in ASDs, we carried out whole-brain iFC analyses for both structural and functional parcellation schemes (that is, structural: Harvard–Oxford Atlas;[34] functional: Crad-200[35]). Whole-brain voxelwise iFC analyses were computationally impractical given the sample size. Beyond whole-brain analyses, we focused on regional voxel-wise measures of intrinsic functional architecture including seed-based iFC of the default network,[26] ReHo,[27,36] VMHC,[37] fALFF[32] and DC.[30,31,38] See Supplementary Information for more details.

Image preprocessing. R-fMRI scans were preprocessed with an alpha version of the Configurable Pipeline for the Analysis of Connectomes (C-PAC, http://fcp-indi.github.com). Image preprocessing steps included slice-timing and motion correction, nuisance signal regression (including six motion parameters, five CompCorr signals[39] and linear trend) and temporal filtering (0.009–0.1 Hz; except for fALFF). Derived R-fMRI measures were normalized to Montreal Neurological Institute (MNI)152 stereotactic space (2 mm^3 isotropic) with linear and non-linear registrations and spatially smoothed (applied full-width at half-maximum = 6 mm). For VMHC analysis, functional data were registered to a symmetric template.

Whole-brain iFC analyses. For each parcellation scheme, we extracted the mean time series for each unit from the preprocessed four-dimensional time series data in MNI space, and then calculated the full-brain connectivity matrix using Pearson's correlation. To ensure normality,

correlation coefficients were Fisher transformed to *Z*-scores. To facilitate data characterization and interpretation, we sorted connections based on lobar (that is, frontal, temporal, parietal, occipital, subcortical) and functional[40] (that is, heteromodal, unimodal, primary somatosensory, paralimbic, limbic, subcortical) classifications. In addition, following prior results,[41] we sorted findings based on hemispheric configuration (intrahemispheric, homotopic, heterotopic) using the structural parcellation (Crad-200 does not provide explicit homotopic regions).

Regional measures. The following voxel-wise regional metrics were generated for each participant: (1) ReHo,[36] which represents the average Kendall's Tau correlation between a given voxel's time series and its 26 adjacent neighbors; (2) VMHC,[37] which represents the correlation between a voxel and its opposite hemisphere counterpart on a symmetric template; (3) fALFF,[32] a frequency domain metric reflecting the ratio between the amplitude of fluctuations in the 0.01–0.1 Hz band and the total amplitude within the sampled periodogram; and (4) DC,[30,31] a measure of the connectome graph indexing the number of direct connections for a given node (voxel).

Default network iFC. To demonstrate the utility of the large-scale aggregate data set in testing existing hypotheses, we conducted a targeted seed-based correlation examination to test previous suggestions of default network hypoconnectivity in ASD.[23,25,42–44] We focused on its

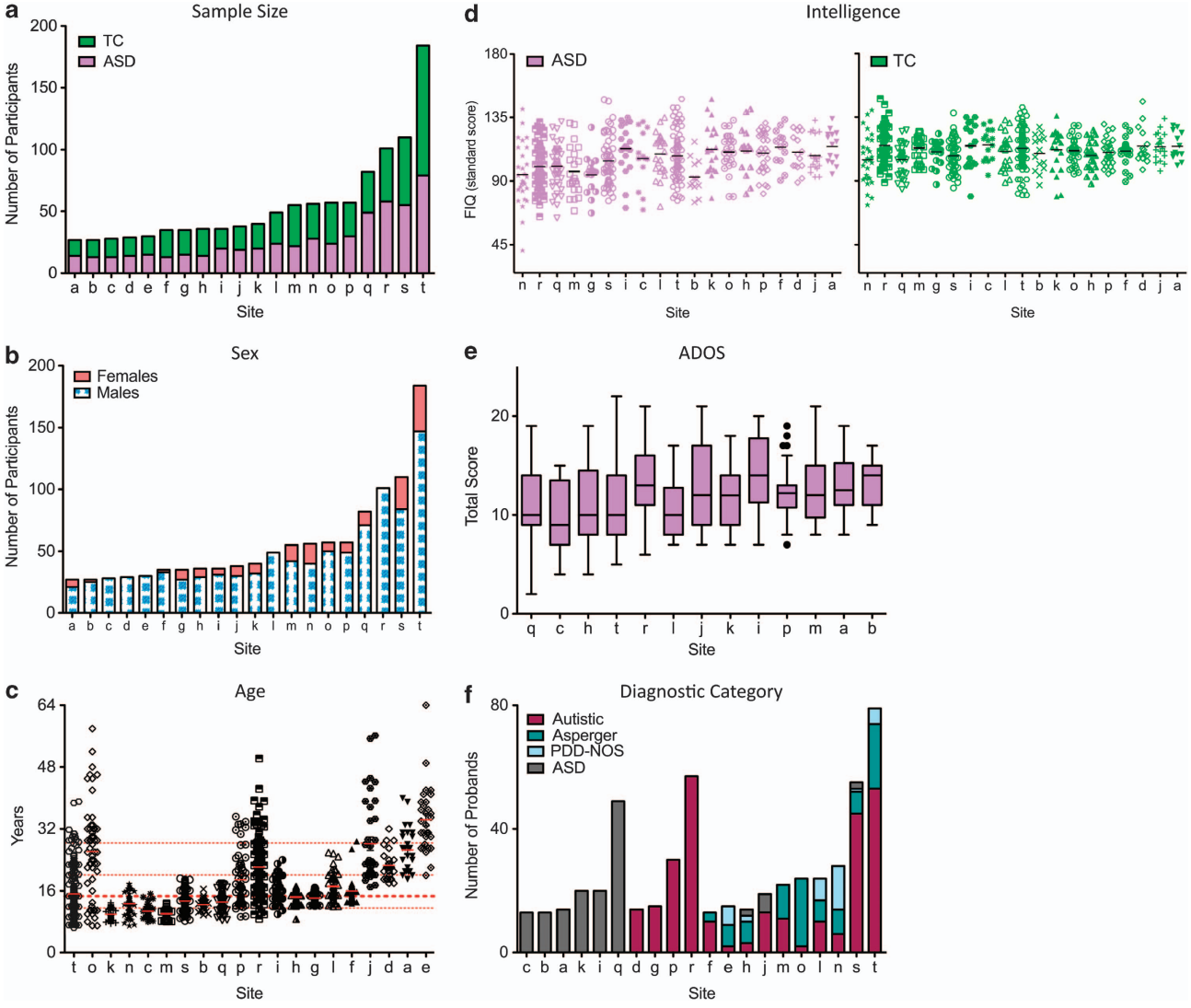

Figure 1. Autism Brain Imaging Data Exchange (ABIDE) sample characteristics. (**a**) Total number of participants per group (green = typical controls (TCs); purple = autism spectrum disorders (ASDs)) for each contributing site ordered as a function of sample size (labeled alphabetically, see Supplementary Table 2 for label key). The same site labels are used for (**b**–**f**). (**b**) Number of male subjects (blue-white) and female subjects (red) for each site irrespective of diagnostic group (groups were matched for sex). (**c**) Age (in years) for all individuals per site (ordered by youngest age included per site) irrespective of diagnostic group (groups were age matched). Each site's mean is represented as a solid red line; the median age across sites (14.7 years) is depicted with a thick red dashed line; 25th, 75th and 90th percentiles (11.7, 20.1 and 28.3 years, respectively) are represented by thin red dashed lines. (**d**) Distribution of full IQ (FIQ) standard scores per site (ordered by lowest FIQ included per site) for individuals with ASDs (purple, left plot) and TCs (green, right plot), respectively. Solid black lines indicate mean FIQ per site. (**e**) The Tukey's box-whiskers plots depict the distribution of Total Autism Diagnostic Observation Scale (ADOS) scores (that is, sum of scaled Communication and Reciprocal Social interaction subtotals) for individuals with ASDs in the 13 sites using the ADOS. (**f**) Number of probands assigned to specific ASD diagnostic categories per site. Categories were DSM-IV-TR (fourth and text revised edition of the Diagnostic and Statistical Manual of Mental Disorders) autistic disorder (red), Asperger syndrome (aqua green), and pervasive developmental disorder-not otherwise specified (PDD-NOS) (light blue) and individuals identified as ASD but not further differentiated into specific DSM-IV-TR subtypes (gray). Data displayed in panel **d** and panel **e** were imputed as described in the main text.

midline core,[26] using spherical region-of-interest masks (radius = 4 mm) centered at anterior medial prefrontal cortex, and posterior cingulate.[26] For each seed region, a Fisher's *Z*-transformed correlation map was generated.

Group-level analyses. We used a general linear model implemented in Data Processing Assistant for Resting-State fMRI (DPARSF)[45] to examine neuroimaging differences related to diagnosis (covariates: age, FIQ, site and mean FD). To correct for multiple comparisons at the cluster level, we employed Gaussian random field theory (voxel $Z > 2.3$, cluster-level $P < 0.05$). For parcellation-based whole-brain correlation analyses, we corrected for multiple comparisons using false discovery rate ($q < 0.05$).[46]

Secondary analyses: 'scrubbed' data. Given the potential for spurious signal changes from head micromovements,[18,33,47–49] primary analyses accounted for group differences in micromovements by covarying for mean FD at the group level.[47] To verify the effectiveness of this approach, we repeated the analyses after removing frames with FD > 0.2 mm ('scrubbing'); individuals with >50% of their time series removed were excluded from the analyses. fALFF was not calculated with 'scrubbed' data as the removal of time points disrupts the temporal structure precluding standard Fourier transform-based approaches.[14]

Structural analyses. Although beyond this work's scope, to demonstrate the ability to conduct structural analyses using ABIDE data sets, we computed total intracranial, white matter, gray matter and cerebrospinal fluid volumes; no significant group differences emerged (Supplementary Figure 2 and Supplementary Information).

RESULTS

Sample composition

Seventeen sites (Figure 1a and Supplementary Table 2) contributed 20 previously collected data sets for 1112 individuals (533 with ASDs, 579 TCs); 10 data sets (58%) were previously unpublished with regard to ASD vs TC R-fMRI comparisons. Contributions per site ranged from 13 to 79 participants with ASDs and 13 to 105 TCs. Marked variation in age range across samples was evident along with a vast predominance of male subjects, with 25% of sites excluding female subjects by design (Figure 1b and Supplementary Table 2). With few exceptions, sites included individuals with average or above-average intelligence. Mean FIQ exceeded 100 for TCs for all sites and in 17 of 20 data sets for individuals with ASDs. Sites varied with respect to the minimum FIQ included (ASDs: 41–95; TCs: 73–101; Figure 1d); FIQ and verbal IQ were significantly greater for TCs than ASDs ($P < 0.0001$) and so was performance IQ, although it only differed marginally ($P = 0.067$). Right-handedness was more frequent in TCs than in ASDs ($P < 0.002$). The male-only sample included for imaging analyses reflected these characteristics (Supplementary Tables 1 and 3).

Sites reached ASD diagnoses by either (1) combining clinical judgment and 'gold standard' diagnostic instruments—Autism Diagnostic Observation Schedule (ADOS) and/or Autism Diagnostic Interview–Revised ($n = 13$ samples, 65% of data sets),[3] (2) clinical judgment only ($n = 3$, 15%) or (3) 'gold standard' diagnostic instruments only ($n = 4$, 20%). Among the 17 sites using the ADOS and/or Autism Diagnostic Interview-Revised, 16 (94%) obtained research-reliable administrations and scorings. Site-specific details are available at http://fcon_1000.projects.nitrc.org/indi/abide. Given participant ages (>6 years) and IQ, most were evaluated with ADOS Modules 3 or 4. Average ADOS total scores were similar across sites, suggesting consistency in ASD severity. Calibrated severity scores (computed using the new ADOS algorithm for Modules 1, 2 and 3)[50] were available for nine sites and confirmed this pattern. DSM-IV-TR diagnostic subtypes were provided by 80% of sites. Consistent with

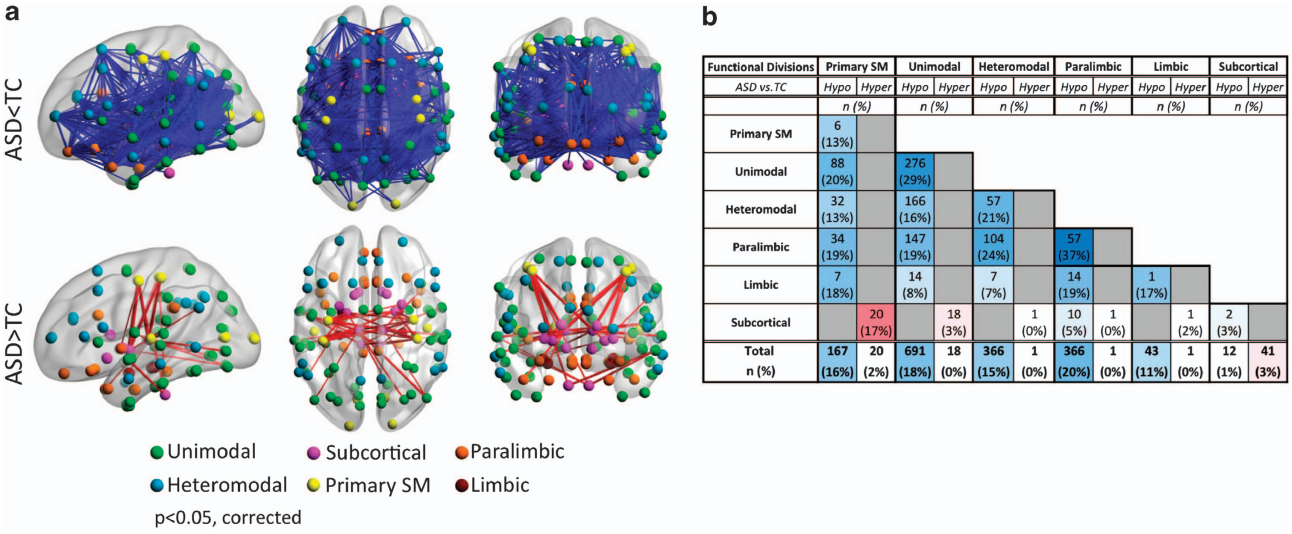

b

Functional Divisions	Primary SM		Unimodal		Heteromodal		Paralimbic		Limbic		Subcortical	
ASD vs.TC	*Hypo*	*Hyper*	*Hypo*	*Hyper*	*Hypo*	*Hyper*	*Hypo*	*Hyper*	*Hypo*	*Hyper*	*Hypo*	*Hyper*
	n (%)		*n (%)*		*n (%)*		*n (%)*		*n (%)*		*n (%)*	
Primary SM	6 (13%)											
Unimodal	88 (20%)		276 (29%)									
Heteromodal	32 (13%)		166 (16%)		57 (21%)							
Paralimbic	34 (19%)		147 (19%)		104 (24%)		57 (37%)					
Limbic	7 (18%)		14 (8%)		7 (7%)		14 (19%)		1 (17%)			
Subcortical		20 (17%)		18 (3%)		1 (0%)	10 (5%)	1 (0%)		1 (2%)	2 (3%)	
Total n (%)	**167 (16%)**	**20 (2%)**	**691 (18%)**	**18 (0%)**	**366 (15%)**	**1 (0%)**	**366 (20%)**	**1 (0%)**	**43 (11%)**	**1 (0%)**	**12 (1%)**	**41 (3%)**

Figure 2. Whole-brain intrinsic functional connectivity analyses. (**a**) Significant group differences (that is, autism spectrum disorders (ASDs) vs typical controls (TCs)) for intrinsic functional connectivity between each of the 112 parcellation units (56 per hemisphere) included in the structural Harvard–Oxford Atlas. Parcellations are represented with their center of mass overlaid as spheres on glass brains. The upper panel shows the intrinsic functional connections (blue lines) that were significantly weaker in ASD vs TC. The lower panel shows the intrinsic functional connections that were significantly stronger in ASD relative to TC (red lines). Each Harvard–Oxford Atlas unit is colored based on its membership in the six functional divisions as per Mesulam *et al.*[44] (yellow = primary sensorimotor (SM); green = unimodal association; blue = heteromodal association; orange = paralimbic; red = limbic; pink = subcortical). Interhemispheric intrinsic functional connectivity is noted on dorsal and coronal views. Glass brains (left lateral, dorsal and coronal views, shown from left to right) are generated using BrainNet Viewer (http://www.nitrc.org/projects/bnv/). Displayed results are corrected for multiple comparisons using false discovery rate at $P < 0.05$. (**b**) The table summarizes the absolute number and percentage of node-to-node intrinsic functional connectivity surviving statistical threshold for group comparisons within and between functional divisions. Gray cells represent the absence of significant intrinsic functional connectivity, blue cells represent ASD-related hypoconnectivity (Hypo: ASD < TC), while red cells represent hyperconnectivity (Hyper: ASD > TC). Blue and red shadings decrease proportionally from the highest percentage (37%) to the lowest (~0%). See Supplementary Tables 4–6 for results based on lobar and hemispheric divisions, as well as for those based on the Crad-200 functional parcellation and Supplementary Information for further discussion on the approach.

previous findings,[3] sites differed substantially in these subtype (autism, Asperger disorder, pervasive developmental disorder not otherwise specified (PDD-NOS)) distributions (Figure 1f and Supplementary Tables 1 and 3).

Imaging findings

Whole-brain iFC. Regardless of parcellation scheme (structural/functional), we found both hypo- and hyperconnectivity in ASDs, although with a striking predominance of hypoconnectivity (Figure 2). Analyses sorting abnormal iFC based on functional hierarchy[40] showed decreased corticocortical iFC across all functional divisions, although in varying degrees (omnibus $\chi^2_4 = 33.5$, $P < 0.0001$), with paralimbic and unimodal association regions having the highest proportions of affected connections (Figure 2 and Supplementary Table 4). Lobar-based classification suggested hypoconnectivity in all lobes, but particularly for the temporal (Supplementary Table 5). ASD-related hyperconnectivity was limited to subcortical regions, particularly for iFC between subcortical (thalamus and globus pallidus) and primary parietal sensorimotor regions (Figure 2 and Supplementary Tables 4 and 5). Finally, examining hemispheric schemes[41] revealed ASD-related iFC decreases particularly in homotopic iFC (Figure 2a, dorsal and coronal views; Supplementary Table 6). This pattern of results remained largely unchanged after 'scrubbing'—consistent with recent work,[18,49] suggesting that including mean FD as a group-level covariate provides findings similar to scrubbing (Supplementary Figure 3 and Supplementary Information).

Regional abnormalities. Figure 3 shows brain regions exhibiting significant group differences in regional metrics. We highlight regions exhibiting convergence in ASD-related differences among measures, suggesting more pervasive disturbances in ASD (Figure 4). Two clusters exhibited ASD-related abnormalities in three measures. The first extended from the left posterior insula to the central and parietal operculum and exhibited ASD-related decreases in VMHC, ReHo and DC. The second cluster was located in right dorsal superior frontal cortex and exhibited ASD-related increases in fALFF, ReHo and DC. A distributed set of regions exhibited ASD-related reductions in at least two measures, including thalamus, posterior cingulate, bilateral mid-insula and left middle occipital gyrus. Again, these findings were largely unchanged after 'scrubbing' (Supplementary Figure 4).

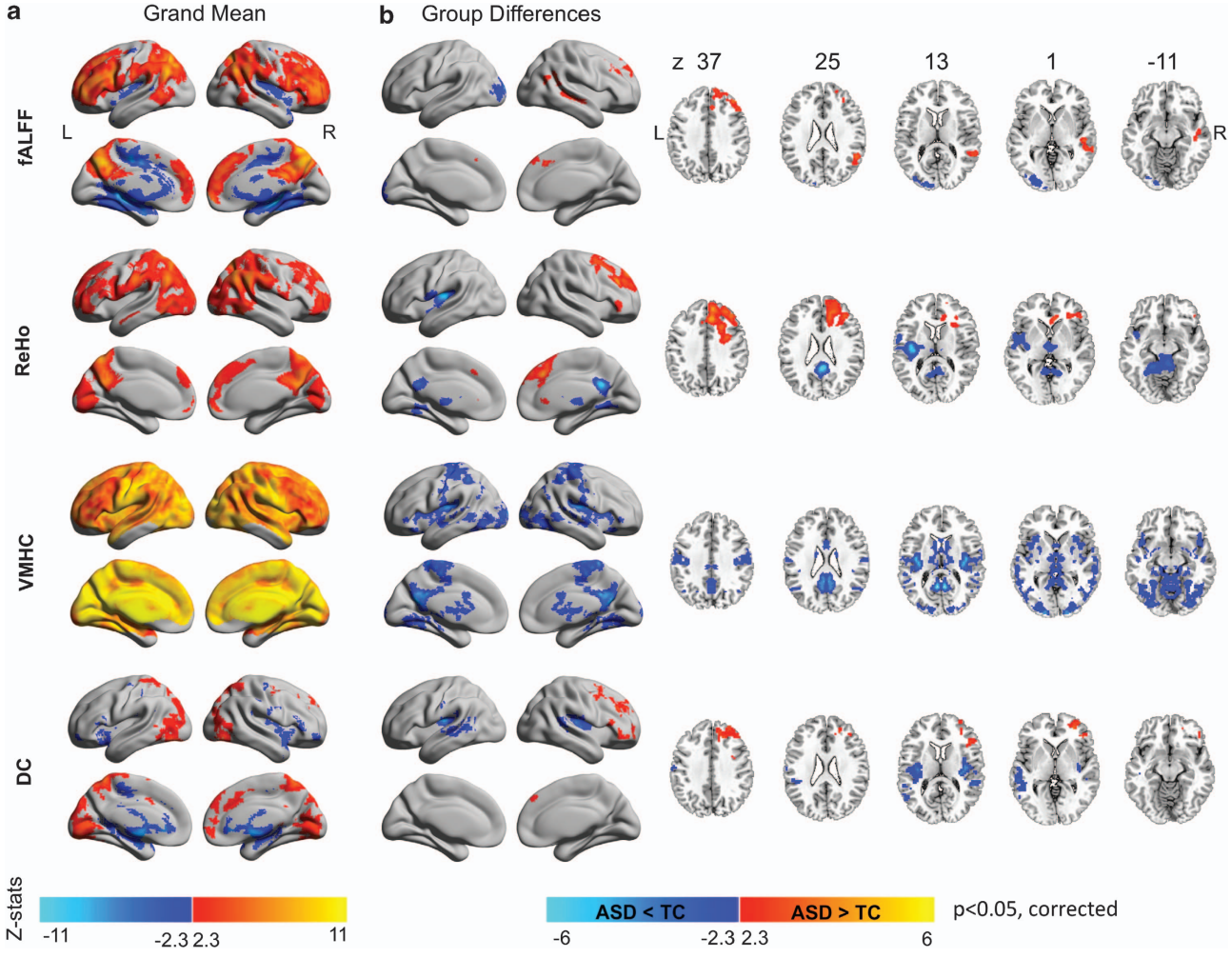

Figure 3. Regional measures of intrinsic functional architecture. (**a**) Z maps of the grand means (that is, across all 763 individuals) and (**b**) significant group differences between individuals with autism spectrum disorders (ASDs) and typical controls (TCs) for each of the four regional measures examined. These were fractional amplitude of low-frequency fluctuations (fALFF), regional homogeneity (ReHo), voxel-mirrored homotopic connectivity (VMHC) and degree centrality (DC). We employed Gaussian random field theory to carry out cluster-level corrections for multiple comparisons (voxel-level $Z > 2.3$; cluster significance: $P < 0.05$, corrected). Significant clusters are overlaid on inflated surface maps generated using BrainNet Viewer (http://www.nitrc.org/projects/bnv/), as well as on axial images generated with REST Slice Viewer (http://www.restfmri.net). L, left hemisphere; R, right hemisphere.

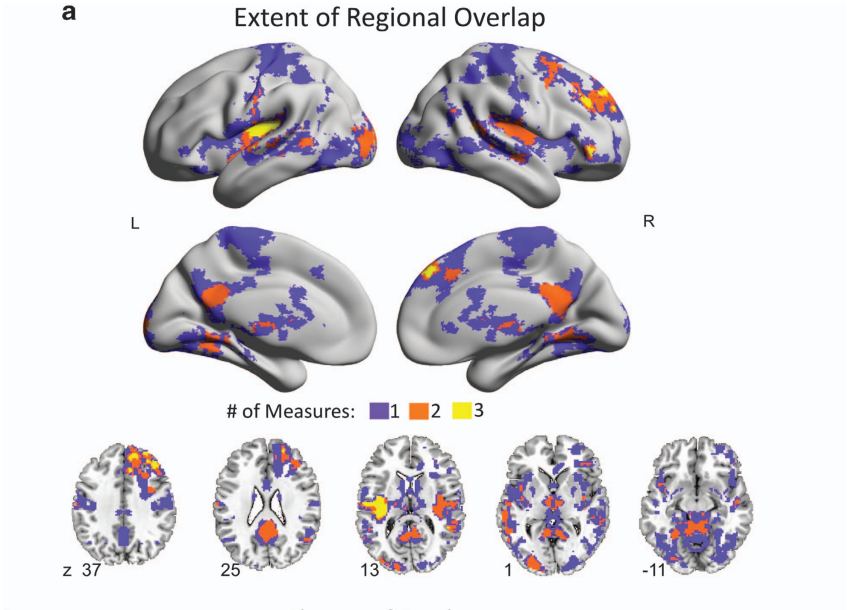

b Clusters of Overlap

Region with Overlap	Cluster size #Voxels	Center of Mass (MNI) x	y	z	Regional Measure fALFF	ReHo	VMHC	DC
Middle Frontal G R	2218	23	31	41				
Insula L	1212	-41	-16	13				
Insula R	644	41	-17	14				
PCC R	2101	1	-50	10				
Occipital Pole L	578	-24	-93	4				
Thalamus L	388	-2	-14	6				
Middle Temporal G L	203	-59	-40	4				

ASD>TC
ASD<TC

Figure 4. Overlap between regional measures of intrinsic brain function. (**a**) Surface and axial maps depict the extent of overlap for significant group differences (that is, autism spectrum disorders (ASDs) vs typical controls (TCs)) among any of the four regional measures of intrinsic brain function shown in Figure 3. Purple clusters represent areas of significant group differences emerging for only one measure; orange and yellow clusters indicate measures with overlap among two and three measures, respectively. (**b**) For each of the yellow and orange clusters shown in panel **a**, the table lists the cluster's anatomical area label, cluster size in the number of voxels and stereotaxic coordinates for the center of mass in Montreal Neurological Institute (MNI) coordinates, the specific measures involved in the overlap, and the group difference direction (ASD > TC in red; ASD < TC in blue). L, left hemisphere; R, right hemisphere.

Focus on the default network. Seed-based correlations confirmed previous findings of ASD-related default network hypoconnectivity.[23,25,42–44] Specifically, we noted decreased long-distance iFC between its anterior and posterior components. We also found decreased iFC between each of the default network components and their neighboring regions (for example, posterior cingulate and precuneus; anterior medial and dorsomedial prefrontal cortex; Figure 5). Decreases in long-distance iFC were robust to the specific motion-correction employed ('scrubbing', group-level correction). In contrast, ASD-related decreases in local iFC were less robust; they were detectable for posterior cingulate, but not for medial prefrontal cortex in secondary analyses using 'scrubbed' data (Supplementary Figure 4).

Site-related variation. On the basis of prior work,[15] the ability to detect ASD-related differences in the ABIDE sample does not imply a lack of site-related variation. Although not a primary focus of this study, we present a demonstration of site-related variation and a parametric analysis of the impact of sample size on detectable differences for a representative finding (that is, left insula VMHC; Supplementary Figures 5 and 6 and Supplementary Information).

Normality. Reflective of common practice, this work used parametric statistics. Supplementary Figure 7 demonstrates regional variation in the degree to which assumptions of normality are maintained. Non-parametric confirmatory analyses conducted at the cluster level supported results of primary analyses (Supplementary Table 7). Future work may benefit from exploring voxel-wise non-parametric approaches, when normality assumptions are violated (Supplementary Figure 8 and Supplementary Information).

DISCUSSION

The feasibility of establishing ABIDE, a collection of 20 mostly unpublished samples from 17 independent sites, testifies to the rapid adoption of R-fMRI approaches to ASD as well as to the benefits of diagnostic harmonization in ASDs. Our initial analyses of the ABIDE R-fMRI data replicate and extend important findings in ASDs, and highlight emerging significant themes that merit further study.

Whole-brain connectivity analyses reconciled seemingly conflicting evidence of hypo- and hyperconnectivity,[20,24,51,52] by revealing both phenomena in ASDs, although to different degrees and with distinct topographies. Specifically, while findings of hyperconnectivity in ASDs were limited and primarily associated with subcortical regions, ASD-related hypoconnectivity dominated corticocortical iFC. Of note, while ASD-related decreases in iFC extended across functional cortical divisions, there was a predilection for unimodal association areas and paralimbic circuits. The prominence of unimodal association areas is in line with the autism literature, which has consistently implicated the

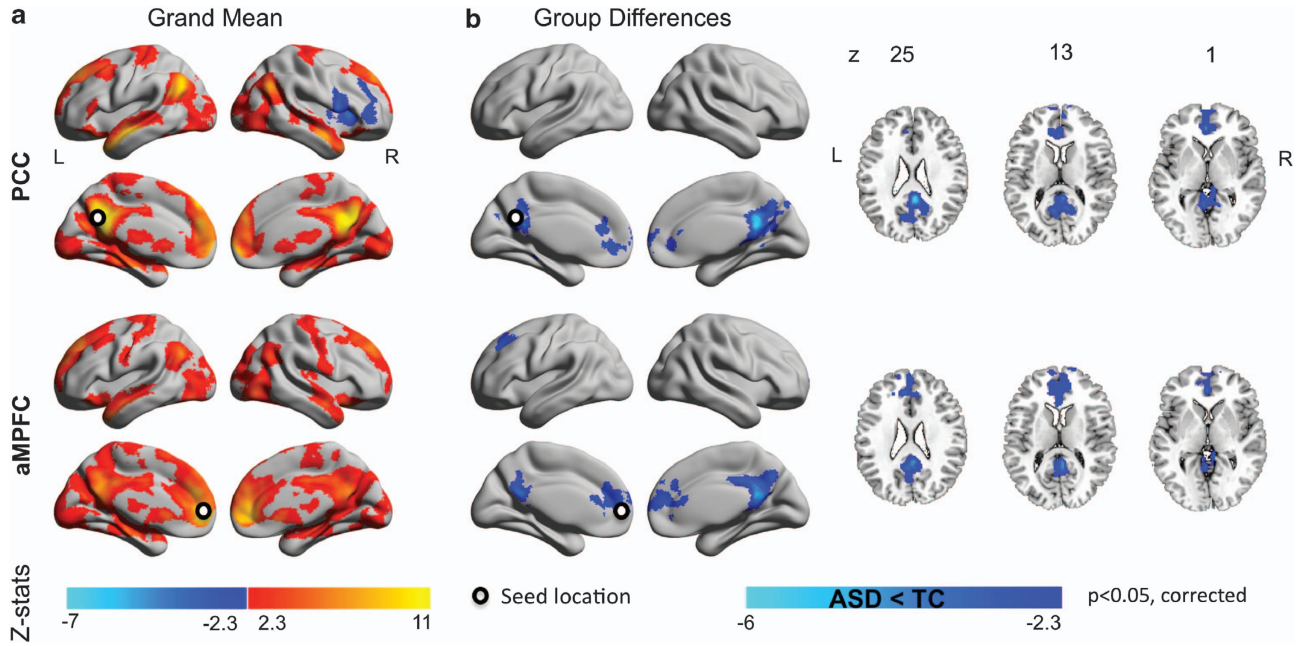

Figure 5. Seed-based correlation analyses: default network. (**a**) Z maps of the grand means (that is, across all 763 individuals) and (**b**) of the group differences between individuals with autism spectrum disorders (ASDs) and typical controls (TCs) for the two midline core seed regions located in posterior cingulate cortex (PCC) and anterior medial prefrontal cortex (aMPFC). Seeds were centered at Montreal Neurological Institute stereotaxic coordinates $x = -8$, $y = -56$, $z = 26$ for PCC and $x = -6$, $y = 52$, $z = -2$ for aMPFC and are depicted as white dots on the surface maps. Gaussian random field theory was used to carry out cluster-level corrections for multiple comparisons (voxel-level $Z > 2.3$; cluster significance: $P < 0.05$, corrected). Significant clusters are overlaid on inflated surface maps generated using BrainNet Viewer (http://www.nitrc.org/projects/bnv/), as well as on axial images generated with REST Slice Viewer (http://www.restfmri.net). L, left hemisphere; R, right hemisphere.

fusiform gyrus,[53] and superior temporal gyrus.[54] Likewise, the implication of paralimbic areas is consistent with studies highlighting ASD-related dysfunction within higher order circuits subserving social, cognitive and affective processes.[21,25] Findings of ASD-related decreases in iFC within the default network midline core further amplify this theme.

Our results also underscore another emerging theme: alterations in interhemispheric connectivity.[10,28,29,55–59] Structural morphometric abnormalities (for example, volume[10,56,57] and microstructure[55,59–61]) in the corpus callosum first drew attention to ASD-related interhemispheric dysconnections. While initial volumetric studies only found evidence of partial compromise of the corpus callosum, diffusion tensor imaging studies of corpus callosum microstructure have suggested abnormalities extending to all major subdivisions.[59,61] Similarly, while initial R-fMRI studies reported abnormalities in interhemispheric iFC for sensorimotor and language areas,[28,29] whole-brain analyses suggest broader compromises, affecting 30% of homotopic connections, across functional hierarchies or lobes. Given that interhemispheric interactions are thought to facilitate high-load cognitive processes,[62] findings of altered connectivity extending across systems may be relevant to models emphasizing impairments of complex reasoning and information processing in ASDs.[63] Intriguingly, this work also highlighted decreases in voxel-wise interhemispheric iFC of subcortical areas, suggesting that callosal abnormalities may not exclusively account for abnormal interhemispheric interactions in ASDs.

A concern in R-fMRI studies is that requirements for *a priori* information (for example, seed specification and number of components in independent component or cluster analyses) influence results. By applying a broad array of unbiased regional metrics, we successfully recapitulated some of the most commonly cited loci of dysfunction (for example, insula[64–66] and PCC[23,42,67–69]). Findings of abnormal iFC also converged on a less commonly considered region—the thalamus. While initial R-fMRI studies tended to focus on large-scale cortico–cortico networks,[23,42] recent work has emphasized examination of subcortical functional circuits (for example, cortico-striato-thalamo-cortical circuitry).[52,70] The role of these circuits in both sensory–motor processes and learning—fundamental mechanisms that may underlie the pervasive clinical impairments in ASDs—makes them appealing targets for future studies. Beyond the added value of extending the scope of circuits examined in ASDs, unprecedented findings of abnormal fALFF in ASDs highlight the need to investigate properties of the intrinsic brain beyond functional connectivity. Supporting this notion, recent work suggests that examination of intrinsic fluctuations in the blood oxygen level-dependent signal may provide a window into more fundamental neuronal signatures of ASDs.[71,72]

Along with the substantial statistical power afforded by the ABIDE aggregate sample, we also note the remaining challenges for the field. In particular, the relationships of IQ to psychiatric disorders and brain structure and function are always complex, and the same holds true for our sample. Across sites, the ASD and TC groups both tended to cluster around the average to above-average range of FIQ; however, marked between-site variation was noted in the range, mean values and s.d.—particularly for individuals with ASDs. Future work will need to attend even more closely to IQ, as R-fMRI studies allow the inclusion of individuals with substantially lower IQ than task-based approaches. Beyond IQ, we observed notable variation in the specific diagnostic subtypes reported across studies. Such heterogeneity in presentations of ASDs must be considered when generalizing findings from an individual study to the larger literature. Revisions proposed for DSM-5 offer the promise of increasing the accuracy with which heterogeneity in ASDs is characterized.[3]

These findings of ASD-related differences in intrinsic functional architecture despite variations in age across sites suggest that some aspects of the neural signatures of ASDs remain constant throughout brain maturation. Yet, mirroring the architectural

properties observed in early childhood,[73] evidence of corticocortical hypoconnectivity and subcorticocortical hyperconnectivity suggest maturational abnormalities in ASDs.[52] As only a few ABIDE sites spanned childhood to middle adulthood, a definitive examination of the developing brain in ASD is beyond the scope of this work. Future efforts need to delve into the ascertainment of the developmental dynamics of autism. Including younger ages is a must for such efforts. A meta-analysis of the task-based autism imaging literature in 2009 found that most studies at the time were conducted in adults.[69] The greater representation of children, albeit above 6, in the ABIDE sample suggests that R-fMRI facilitates the examination of neural circuitry at younger ages. Still, the first 6 years of life represent a critical period in neurodevelopment. Further, initial presentations and diagnosis of ASD extend down to as early as 24 months. With rare exceptions,[28,74] early development is poorly represented in the neuroimaging literature. As the field moves towards a more comprehensive understanding of the neural basis of ASD and their developmental trajectories, a shift towards imaging toddlers and preschoolers is unavoidable—particularly if imaging is to strive for clinical utility.

Future efforts should also focus on standardized phenotyping, including and extending diagnostic assessments. This will allow comprehensive characterization of dimensional brain–behavior relationships. In addition, physiologic measurements capable of indexing ASD-related abnormalities in brain function should be considered (for example, eye tracking). Finally, it must be acknowledged that while studies establishing the test–retest reliability for R-fMRI have alleviated concerns about the uncontrolled nature of rest,[12] potential concerns remain that group differences in mental states associated with the magnet environment (for example, anxiety) can contribute to findings. Future efforts examining the unique signatures of differing mental states in R-fMRI data should be encouraged.

In summary, the construction and open release of the ABIDE sample represents a landmark milestone in autism imaging. Bringing together international data sets, the ABIDE sample allows for replication, secondary analyses and discovery efforts, as demonstrated in this work, and provides insights into study designs for the next generation of investigations using multi-faceted databases such as NDAR rapidly growing in size.[75]

CONFLICT OF INTEREST

Catherine Lord receives royalties from the publication of the Autism Diagnostic Interview-Revised and the Autism Diagnostic Observation Schedule. The other authors declare no conflict of interest.

ACKNOWLEDGEMENTS

We thank the numerous contributors at each site (see Supplementary Table 2 and http://fcon_1000.projects.nitrc.org/indi/abide/), particularly Drs Marlene Behrmann and Leonardo Cerliani for their efforts in the collection, organization and sharing of their data sets; the NITRC (http://www.nitrc.org) for providing the data sharing platform for the ABIDE initiative as well as the other informatics databases for providing additional platforms (see http://fcon_1000.projects.nitrc.org/indi/abide). We also thank Ranjit Khanuja and Sharad Sikka for programming support; Dr R Cameron Craddock for invaluable suggestions regarding data analysis, as well as oversight of the development of the Configurable Pipeline for the Analysis of Connectomes, and Drs Zhen Yang and Clare Kelly for suggestions on earlier versions of this manuscript. Support for ABIDE coordination and data aggregation was partially provided by NIMH (K23MH087770, R03MH09632 and BRAINSRO1MH094639-01), the Leon Levy Foundation and by gifts from Joseph P Healey and the Stavros Niarchos Foundation. Support for data collection at each site was provided by NIH (DC011095, MH084164, K01MH092288-Stanford; HD55748, KO1MH081191, MH67924-Pitt; K08MH092697, P50MH60450, R01NS34783, R01MH080826, T32DC008553-USM; K23MH087770, R01HD065282, R01MH081218, R21MH084126-NYU; MH066496, R21MH079871, U19HD035482-UM1&UM2; R00MH091238, R01MH086654, R01MH096773-OHSU; R01MH081023-SDSU; 1R01HD06528001-UCLA1 and -UCLA2; K01MH071284-Yale; R01MH080721; K99/R00MH094409-Caltech), Autism Speaks (KKI, NYU, Olin, UM1 and 2, Pitt, USM, Yale), NINDS (R01NS048527; KKI), NICHD (Yale) NICHD (P50 HD055784; UCLA1 and 2), NICHD/NIDCD (P01/U19; CMU) the Simons Foundation (OHSU, Yale, Caltech, CMU), the Belgian Interuniversity Attraction Poles Grant (P6/29; Leuven 1 and 2), Ben B and Iris M Margolis Foundation (USM), European Commission, Marie Curie Excellence Grant (MEXT-CT-2005-023253; SBL), Flanders Fund for Scientific Research (1841313N, G.0354.06, G.0758.10; and post-doc grant; Leuven 1 and 2), Hartford Hospital (Olin), John Merck Scholars Fund (Yale), Kyulan Family Foundation (Trinity), Michigan Institute for Clinical and Health Research (MICHR) Predoctoral Fellowship (UM1 and 2), The Meath Foundation, Adelaide & Meath Hospital, Dublin Incorporating the National Children's Hospital (AMNCH; Trinity), National Initiative for Brain and Cognition NIHC HCMI (056-13-014, 056-13-017; SBL), NWO (051.07.003, 452-04-305, 400-08-089; SBL) and Netherlands Brain Foundation (KS 2010(1)-29; SBL), NRSA Pre-doctoral Fellowship (F31DC010143; USM), Research Council of the University of Leuven (Leuven 1 and 2), Singer Foundation and Stanford Institute for Neuro-Innovations and Translational Neurosciences (Stanford), Leon Levy Foundation (NYU), Stavros Niarchos Foundation (NYU), UCLA Autism Center of Excellence (UCLA1 and 2), Autism Science Foundation (Yale) and University of Utah Multidisciplinary Research Seed Grant (USM).

REFERENCES

1 Centers for Disease Control and Prevention. Prevalence of autism spectrum disorders — autism and developmental disabilities monitoring network, 14 sites, United States, 2008. *MMWR Surveill Summ* 2012; **61**: 1–19.
2 Kim YS, Leventhal BL, Koh YJ, Fombonne E, Laska E, Lim EC *et al.* Prevalence of autism spectrum disorders in a total population sample. *Am J Psychiatry* 2011; **168**: 904–912.
3 Lord C, Petkova E, Hus V, Gan W, Lu F, Martin DM *et al.* A multisite study of the clinical diagnosis of different autism spectrum disorders. *Arch Gen Psychiatry* 2012; **69**: 306–313.
4 Lord C, Risi S, Lambrecht L, Cook EH, Leventhal BL, DiLavore PC *et al.* The Autism Diagnostic Observation Schedule-Generic: A standard measure of social and communication deficits associated with the spectrum of autism. *Journal of Autism and Developmental Disorders* 2000; **30**: 205–223.
5 Geschwind DH, Sowinski J, Lord C, Iversen P, Shestack J, Jones P *et al.* The autism genetic resource exchange: a resource for the study of autism and related neuropsychiatric conditions. *Am J Hum Genet* 2001; **69**: 463–466.
6 Moreno-De-Luca D, Sanders SJ, Willsey AJ, Mulle JG, Lowe JK, Geschwind DH *et al.* Using large clinical data sets to infer pathogenicity for rare copy number variants in autism cohorts. *Mol Psychiatry* advance online publication, 9 October 2012; doi:10.1038/mp.2012.138 (e-pub ahead of print).
7 Fischbach GD, Lord C. The Simons Simplex Collection: a resource for identification of autism genetic risk factors. *Neuron* 2010; **68**: 192–195.
8 Szatmari P, Paterson AD, Zwaigenbaum L, Roberts W, Brian J, Liu XQ *et al.* Mapping autism risk loci using genetic linkage and chromosomal rearrangements. *Nat Genet* 2007; **39**: 319–328.
9 Minshew NJ, Williams DL. The new neurobiology of autism: cortex, connectivity, and neuronal organization. *Arch Neurol* 2007; **64**: 945–950.
10 Just MA, Cherkassky VL, Keller TA, Minshew NJ. Cortical activation and synchronization during sentence comprehension in high-functioning autism: evidence of underconnectivity. *Brain* 2004; **127**(Part 8): 1811–1821.
11 Vissers ME, Cohen MX, Geurts HM. Brain connectivity and high functioning autism: a promising path of research that needs refined models, methodological convergence, and stronger behavioral links. *Neurosci Biobehav Rev* 2012; **36**: 604–625.
12 Shehzad Z, Kelly AM, Reiss PT, Gee DG, Gotimer K, Uddin LQ *et al.* The resting brain: unconstrained yet reliable. *Cereb Cortex* 2009; **19**: 2209–2229.
13 Van Dijk KR, Hedden T, Venkataraman A, Evans KC, Lazar SW, Buckner RL. Intrinsic functional connectivity as a tool for human connectomics: theory, properties, and optimization. *J Neurophysiol* 2010; **103**: 297–321.
14 Kelly C, Biswal BB, Craddock RC, Castellanos FX, Milham MP. Characterizing variation in the functional connectome: promise and pitfalls. *Trends Cogn Sci* 2012; **16**: 181–188.
15 Biswal BB, Mennes M, Zuo XN, Gohel S, Kelly C, Smith SM *et al.* Toward discovery science of human brain function. *Proc Natl Acad Sci USA* 2010; **107**: 4734–4739.
16 Mennes M, Biswal B, Castellanos FX, Milham MP. Making data sharing work: the FCP/INDI experience. *NeuroImage* advance online publication, 30 October 2012; doi:10.1016/j.neuroimage.2012.10.064 (e-pub ahead of print).
17 ADHD-200 Consortium. The ADHD-200 Consortium: a model to advance the translational potential of neuroimaging in clinical neuroscience. *Front Syst Neurosci* 2012; **6**: 1–5.
18 Fair DA, Nigg JT, Iyer S, Bathula D, Mills KL, Dosenbach NU *et al.* Distinct neural signatures detected for ADHD subtypes after controlling for micro-movements in resting state functional connectivity MRI data. *Front Syst Neurosci* 2012; **6**: 80.
19 Tomasi D, Volkow ND. Abnormal functional connectivity in children with attention-deficit/hyperactivity disorder. *Biol Psychiatry* 2012; **71**: 443–450.

20 Muller RA, Shih P, Keehn B, Deyoe JR, Leyden KM, Shukla DK. Underconnected, but how? A survey of functional connectivity MRI studies in autism spectrum disorders. *Cereb Cortex* 2011; **21**: 2233–2243.
21 Gotts SJ, Simmons WK, Milbury LA, Wallace GL, Cox RW, Martin A. Fractionation of social brain circuits in autism spectrum disorders. *Brain* 2012; **135**(Part 9): 2711–2725.
22 Kennedy DP, Redcay E, Courchesne E. Failing to deactivate: resting functional abnormalities in autism. *Proc Natl Acad Sci USA* 2006; **103**: 8275–8280.
23 Assaf M, Jagannathan K, Calhoun VD, Miller L, Stevens MC, Sahl R *et al.* Abnormal functional connectivity of default mode sub-networks in autism spectrum disorder patients. *NeuroImage* 2010; **53**: 247–256.
24 Monk CS, Peltier SJ, Wiggins JL, Weng SJ, Carrasco M, Risi S *et al.* Abnormalities of intrinsic functional connectivity in autism spectrum disorders. *NeuroImage* 2009; **47**: 764–772.
25 Rudie JD, Shehzad Z, Hernandez LM, Colich NL, Bookheimer SY, Iacoboni M *et al.* Reduced functional integration and segregation of distributed neural systems underlying social and emotional information processing in autism spectrum disorders. *Cereb Cortex* 2012; **22**: 1025–1037.
26 Andrews-Hanna JR, Reidler JS, Sepulcre J, Poulin R, Buckner RL. Functional-anatomic fractionation of the brain's default network. *Neuron* 2010; **65**: 550–562.
27 Paakki JJ, Rahko J, Long X, Moilanen I, Tervonen O, Nikkinen J *et al.* Alterations in regional homogeneity of resting-state brain activity in autism spectrum disorders. *Brain Res* 2010; **1321**: 169–179.
28 Dinstein I, Pierce K, Eyler L, Solso S, Malach R, Behrmann M *et al.* Disrupted neural synchronization in toddlers with autism. *Neuron* 2011; **70**: 1218–1225.
29 Anderson JS, Druzgal TJ, Froehlich A, DuBray MB, Lange N, Alexander AL *et al.* Decreased interhemispheric functional connectivity in autism. *Cereb Cortex* 2011; **21**: 1134–1146.
30 Zuo XN, Ehmke R, Mennes M, Imperati D, Castellanos FX, Sporns O *et al.* Network centrality in the human functional connectome. *Cereb Cortex* 2012; **22**: 1862–1875.
31 Buckner RL, Sepulcre J, Talukdar T, Krienen FM, Liu H, Hedden T *et al.* Cortical hubs revealed by intrinsic functional connectivity: mapping, assessment of stability, and relation to Alzheimer's disease. *J Neurosci* 2009; **29**: 1860–1873.
32 Zuo XN, Di Martino A, Kelly C, Shehzad ZE, Gee DG, Klein DF *et al.* The oscillating brain: complex and reliable. *NeuroImage* 2010; **49**: 1432–1445.
33 Power JD, Barnes KA, Snyder AZ, Schlaggar BL, Petersen SE. Spurious but systematic correlations in functional connectivity MRI networks arise from subject motion. *NeuroImage* 2012; **59**: 2142–2154.
34 Kennedy DN, Lange N, Makris N, Bates J, Meyer J, Caviness Jr VS. Gyri of the human neocortex: an MRI-based analysis of volume and variance. *Cereb Cortex* 1998; **8**: 372–384.
35 Craddock RC, James GA, Holtzheimer III PE, Hu XP, Mayberg HS. A whole brain fMRI atlas generated via spatially constrained spectral clustering. *Hum Brain Mapp* 2012; **33**: 1914–1928.
36 Zang Y, Jiang T, Lu Y, He Y, Tian L. Regional homogeneity approach to fMRI data analysis. *NeuroImage* 2004; **22**: 394–400.
37 Zuo XN, Kelly C, Di Martino A, Mennes M, Margulies DS, Bangaru S *et al.* Growing together and growing apart: regional and sex differences in the lifespan developmental trajectories of functional homotopy. *J Neurosci* 2010; **30**: 15034–15043.
38 Bullmore E, Sporns O. Complex brain networks: graph theoretical analysis of structural and functional systems. *Nat Rev Neurosci* 2009; **10**: 186–198.
39 Behzadi Y, Restom K, Liau J, Liu TT. A component based noise correction method (CompCor) for BOLD and perfusion based fMRI. *NeuroImage* 2007; **37**: 90–101.
40 Mesulam MM. From sensation to cognition. *Brain* 1998; **121**(Part 6): 1013–1052.
41 Stark DE, Margulies DS, Shehzad ZE, Reiss P, Kelly AM, Uddin LQ *et al.* Regional variation in interhemispheric coordination of intrinsic hemodynamic fluctuations. *J Neurosci* 2008; **28**: 13754–13764.
42 Cherkassky VL, Kana RK, Keller TA, Just MA. Functional connectivity in a baseline resting-state network in autism. *NeuroReport* 2006; **17**: 1687–1690.
43 Weng SJ, Wiggins JL, Peltier SJ, Carrasco M, Risi S, Lord C *et al.* Alterations of resting state functional connectivity in the default network in adolescents with autism spectrum disorders. *Brain Res* 2010; **1313**: 202–214.
44 Jones TB, Bandettini PA, Kenworthy L, Case LK, Milleville SC, Martin A *et al.* Sources of group differences in functional connectivity: an investigation applied to autism spectrum disorder. *NeuroImage* 2010; **49**: 401–414.
45 Yan C, Yu-Feng Z. DPARSF: a MATLAB toolbox for 'pipeline' data analysis of resting-state fMRI. *Front Syst Neurosci* 2010; **4**: 13.
46 Genovese CR, Lazar NA, Nichols T. Thresholding of statistical maps in functional neuroimaging using the false discovery rate. *NeuroImage* 2002; **15**: 870–878.
47 Van Dijk KR, Sabuncu MR, Buckner RL. The influence of head motion on intrinsic functional connectivity MRI. *NeuroImage* 2012; **59**: 431–438.
48 Satterthwaite TD, Wolf DH, Loughead J, Ruparel K, Elliott MA, Hakonarson H *et al.* Impact of in-scanner head motion on multiple measures of functional connectivity: relevance for studies of neurodevelopment in youth. *NeuroImage* 2012; **60**: 623–632.
49 Yan C, Cheung B, Kelly C, Colcombe S, Craddock C, Di Martino A *et al.* Comprehensive assessment of regional variation in the impact of head micromovements on functional connectomics. *NeuroImage* 2013; **76**: 183–201.
50 Gotham K, Pickles A, Lord C. Standardizing ADOS scores for a measure of severity in autism spectrum disorders. *J Autism Dev Disord* 2009; **39**: 693–705.
51 Just MA, Keller TA, Malave VL, Kana RK, Varma S. Autism as a neural systems disorder: a theory of frontal-posterior underconnectivity. *Neurosci Biobehav Rev* 2012; **36**: 1292–1313.
52 Di Martino A, Kelly C, Grzadzinski R, Zuo XN, Mennes M, Mairena MA *et al.* Aberrant striatal functional connectivity in children with autism. *Biol Psychiatry* 2011; **69**: 847–856.
53 Schultz RT, Gauthier I, Klin A, Fulbright RK, Anderson AW, Volkmar F *et al.* Abnormal ventral temporal cortical activity during face discrimination among individuals with autism and Asperger syndrome. *Arch Gen Psychiatry* 2000; **57**: 331–340.
54 Kaiser MD, Hudac CM, Shultz S, Lee SM, Cheung C, Berken AM *et al.* Neural signatures of autism. *Proc Natl Acad Sci USA* 2010; **107**: 21223–21228.
55 Lewis JD, Theilmann RJ, Fonov V, Bellec P, Lincoln A, Evans AC *et al.* Callosal fiber length and interhemispheric connectivity in adults with autism: brain overgrowth and underconnectivity. *Hum Brain Mapp* 2013; doi:10.1002/hbm.22018 (e-pub ahead of print).
56 Hardan AY, Pabalan M, Gupta N, Bansal R, Melhem NM, Fedorov S *et al.* Corpus callosum volume in children with autism. *Psychiatry Res* 2009; **174**: 57–61.
57 Piven J, Bailey J, Ranson BJ, Arndt S. An MRI study of the corpus callosum in autism. *Am J Psychiatry* 1997; **154**: 1051–1056.
58 Cheon KA, Kim YS, Oh SH, Park SY, Yoon HW, Herrington J *et al.* Involvement of the anterior thalamic radiation in boys with high functioning autism spectrum disorders: a diffusion tensor imaging study. *Brain Res* 2011; **1417**: 77–86.
59 Shukla DK, Keehn B, Lincoln AJ, Muller RA. White matter compromise of callosal and subcortical fiber tracts in children with autism spectrum disorder: a diffusion tensor imaging study. *J Am Acad Child Adolesc Psychiatry* 2010; **49**: 1269–12781278 and 1261–1262.
60 Hong S, Ke X, Tang T, Hang Y, Chu K, Huang H *et al.* Detecting abnormalities of corpus callosum connectivity in autism using magnetic resonance imaging and diffusion tensor tractography. *Psychiatry Res* 2011; **194**: 333–339.
61 Alexander AL, Lee JE, Lazar M, Boudos R, Dubray MB, Oakes TR *et al.* Diffusion tensor imaging of the corpus callosum in autism. *NeuroImage* 2007; **34**: 61–73.
62 Banich MT. The missing link: the role of interhemispheric interaction in attentional processing. *Brain Cogn* 1998; **36**: 128–157.
63 Minshew NJ, Goldstein G, Siegel DJ. Neuropsychologic functioning in autism: profile of a complex information processing disorder. *J Int Neuropsychol Soc* 1997; **3**: 303–316.
64 Uddin LQ, Menon V. The anterior insula in autism: under-connected and under-examined. *Neurosci Biobehav Rev* 2009; **33**: 1198–1203.
65 Ebisch SJ, Gallese V, Willems RM, Mantini D, Groen WB, Romani GL *et al.* Altered intrinsic functional connectivity of anterior and posterior insula regions in high-functioning participants with autism spectrum disorder. *Hum Brain Mapp* 2011; **32**: 1013–1028.
66 Di Martino A, Shehzad Z, Kelly C, Roy AK, Gee DG, Uddin LQ *et al.* Relationship between cingulo-insular functional connectivity and autistic traits in neurotypical adults. *Am J Psychiatry* 2009; **166**: 891–899.
67 Kennedy DP, Courchesne E. Functional abnormalities of the default network during self- and other-reflection in autism. *Soc Cogn Affect Neurosci* 2008; **3**: 177–190.
68 Kennedy DP, Courchesne E. The intrinsic functional organization of the brain is altered in autism. *NeuroImage* 2008; **39**: 1877–1885.
69 Di Martino A, Ross K, Uddin LQ, Sklar AB, Castellanos FX, Milham MP. Functional brain correlates of social and nonsocial processes in autism spectrum disorders: an activation likelihood estimation meta-analysis. *Biol Psychiatry* 2009; **65**: 63–74.
70 Mizuno A, Villalobos ME, Davies MM, Dahl BC, Muller RA. Partially enhanced thalamocortical functional connectivity in autism. *Brain Res* 2006; **1104**: 160–174.
71 Lai MC, Lombardo MV, Chakrabarti B, Sadek SA, Pasco G, Wheelwright SJ *et al.* A shift to randomness of brain oscillations in people with autism. *Biol Psychiatry* 2010; **68**: 1092–1099.
72 Dinstein I, Heeger DJ, Lorenzi L, Minshew NJ, Malach R, Behrmann M. Unreliable evoked responses in autism. *Neuron* 2012; **75**: 981–991.
73 Supekar K, Musen M, Menon V. Development of large-scale functional brain networks in children. *PLoS Biol* 2009; **7**: e1000157.
74 Redcay E, Courchesne E. Deviant functional magnetic resonance imaging patterns of brain activity to speech in 2–3-year-old children with autism spectrum disorder. *Biol Psychiatry* 2008; **64**: 589–598.
75 Hall D, Huerta MF, McAuliffe MJ, Farber GK. Sharing heterogeneous data: the national database for autism research. *Neuroinformatics* 2012; **10**: 331–339.

Supplementary Information accompanies the paper on the Molecular Psychiatry website (http://www.nature.com/mp)